Peer-to-Peer Networking and Applications
https://doi.org/10.1007/s12083-020-01003-3

Deep learning based modulation classification for 5G and beyond wireless systems

J. Christopher Clement[1] · N. Indira[1] · P. Vijayakumar[2] · R. Nandakumar[3]

Received: 2 May 2020 / Accepted: 11 September 2020
© Springer Science+Business Media, LLC, part of Springer Nature 2020

Abstract

The 5G and beyond wireless networks will be more dynamic and heterogeneous, which needs to work on multistrand waveforms. One of the most significant challenges in such a dynamic network, especially non cooperated cases, is the identification of particular modulation type, which the transmitter uses at the given time to decode the data successfully. This research proposes a modulation classification algorithm using the combination architectures of modified convolutional neural network. The proposed deep learning architecture is developed by combining the convolutional neural network, dense network, and long short-term memory network (LSTM), which is named as convolutional LSTM dense neural network (CLDNN). Moreover, the mean cumulative sum metric (MCS) is introduced in the pooling layer for improved classification accuracy. Dimensionality reduction through Principal Component Analysis is also applied to minimize the training time, so that the proposed architecture can be adopted for its practical usage. The simulation results prove that the presented CLDNN outperforms an ordinary CNN, while taking less training time.

Keywords Convolutional neural network · Dense network · LSTM · Modulation classification

1 Introduction

Automatic modulation classification is used at the receiver to classify the modulation type of the signal that was transmitted. Typical modulation classification requires expert signal processing algorithms that perform noise reduction and estimation of signal parameters, namely, carrier frequency and signal power. In general, the classification algorithms can be of

- Likelihood based (LB)
- Feature based (FB)
- Artificial Neural Networks based

In LB [22, 25, 26] and FB [6, 9, 27] techniques, the decision threshold is chosen manually, while in the Artificial Neural Network based techniques [15, 16, 19], the threshold is determined adaptively and automatically. In other words, LB algorithms compare the likelihood ratio of each possible hypothesis against a threshold, which is derived from the probability density function of the observed wave.

The deep neural networks, which is built in terms of Convolutional Neural Network (CNN) can successfully classify various numbers of modulation types [20]. The performance characteristics of CNN not only gives better accuracy, but is also flexible in detecting the various modulation types compared to other approaches. Moreover, deep learning applications show remarkable progress in image recognition, 3D action recognition [11], node localization and classification problems. To further the

This article is part of the Topical Collection: *Special Issue on P2P Computing for Beyond 5G Network and Internet-of-Everything*
Guest Editors: Prakasam P, Ajayan John, Shohel Sayeed

✉ J. Christopher Clement
christopher.clement@vit.ac.in

N. Indira
indira.n2018@vitstudent.ac.in

P. Vijayakumar
vijayakp@srmist.edu.in

R. Nandakumar
drrnandakumar@gmail.com

[1] School of Electronics Engineering, Vellore Institute of Technology, Vellore, India

[2] Department of Electronics and Communication Engineering, SRM Institute of Science and Technology, Chennai, India

[3] Department of Electronics and Communication Engineering, K.S.R. Institute for Engineering and Technology, Tamil Nadu, India

Published online: 06 October 2020

improvements, the Residual Neural Network (ResNet) [7] and Densely connected Network (DenseNet) are used [23]. In these networks, the different layers are connected through shortcuts to strengthen the feature propagation. The performance of DenseNet in image recognition is very much appreciated. So, we would like to adapt it for modulation classification.

To minimize the block error rate, beyond 5G wireless system's base station adapts appropriate modulation scheme in accordance with the variations in channel state [2]. In 5G and beyond wireless networks, the receiver seems to use a different modulation type than the one which is used by the transmitter.

In the latest 5G standards, as the receiver receives signals from multiple directions and sources, there is a possibility of multipath fading, which leads to the difficulty in identifying the signal at the receiver side [29]. In beyond 5G communication systems, this problem becomes worse, as there are a massive number of multiple input and output antennas used by the receiver. This massive number of antennas lets the receiver receive signals from many other sources in all directions. So, a real life system to categorize the modulation at the receiver is needed.

There are a few algorithms reported for the automatic modulation classification [1, 3, 17]. However, most of the reported works concentrated on the accuracy, but not on the time taken for classification. If a considerable amount of time is utilized for classification, then the latency requirements for higher standard communications will not be met. The latency standard for 5G networks is defined in [21]. In [10], it is reported that the required latency is of the degree of 0.1 ms. However, for the modulation categorization, the latency is required to be 90% lesser, meaning that on the order of 0.01 ms. To achieve this standard, and high accuracy, artificial intelligence is used in modulation classifications.

We organise the paper in this way. In Section 3, we present the CLDNN based modulation classification with MCS pooling and the dimensionality reduction using PCA. Section 4 describes about dataset and training. The results are discussed in Sections 5 and 6 concludes the work.

2 Related work

A modulation classification work for fifth generation (5G) network and unmanned aerial vehicle (UAV) is proposed [14] to classify the modulation type in presence of multipath fading. The algorithm can perform classification without any prior information about multipath channel. The algorithm compute wavelet transform then it uses mean, variance, skewness and kurtosis of the transformed value as feature vector. The principal component analysis (PCA) is used for feature selection and neural network is used as classifier.

Another modulation classification using Extreme Learning Machine (ELM) as a classifier is presented [5]. The work uses Local Binary Pattern (LBP) as feature set. Author's contribution in this work is its ability of quick classification and its better generalization. Authors have also analysed the stability with respect to the variation in the parameters like the roll-off factor, frequency and phase offset.

An automatic modulation classification system for Space-Time-Block-Codes (STBC)-MIMO systems Multiple-Input Multiple-Output (MIMO) is proposed with deep neural network [24]. Sparse Autoencoders (SAE) and Radial Basis Function Network (RBFN) are used as classifiers. Limited-memory Broyden-Fletcher-Goldfarb-Shanno(L-BFGS) and the least square method is used as an optimizer. The analysis of the impact of channel estimation error on the classification performance is also carried out in the work. The performance analysis carried out for perfect channel state information (CSI) and blind case with channel estimation error.

A modulation signal classification system which uses combining Neutrosophic c-means (NCM) based feature weighting (NCMBFW) and classifier algorithms is proposed for multi-carrier signal [4]. The multi-carrier amplitude shift keying (MC-ASK), frequency shift keying (MC-FSK), and phase shift keying (MC-PSK) modulation types are tested. The different domain features like time, frequency, and time-frequency are extracted and those features are weighted by NCMBFW method. Various classifiers namely Linear Discriminant Analysis (LDA), Support Vector Machine (SVM), k-nearest neighbor (k-NN), AdaBoostM1, and Random Forest are used as classifiers.

Deep learning algorithms require large data set to provide better classification performance. But in many practical scenarios, only a small sample set (SSS) will be available. To overcome this issue, a new classification work which can take only a few data set that too using low SNR samples is proposed by [30]. A modulated autocorrelation convolution networks (MACNs) is proposed to solve the problem in which signals are classified with the periodic local features by applying an autocorrelation convolution criterion. Modulation filters are used to improve the capacity of the convolution filters. It has inherent compression mechanism while reduces required storage space of convolutional filters by a factor of eight.

Another deep learning based modulation classification for multiple-input multiple-output (MIMO) systems is proposed using a convolutional neural network (CNN) [28]. The method is designed as cooperative automatic modulation classification for the MIMO systems, where the cooperation is established between the multiple antennas located in the classifying receiver. In the scheme, each

receiver antenna creates sub results, which are then combined by a decision maker to create final classification output. Direct voting (DV), weighty voting (WV), direct averaging (DA) and weighty averaging (WA) are used as a combiner at the decision maker. Among these combiners, WA provided highest correct classification.

In this paper, we implement a CLDNN, the combination of CNN, LSTM and densenet, for modulation classification. In our proposed network, the memory unit present in the LSTM is expected to increase the classification accuracy, on the other hand the densenet architecture reduces latency. To further reduce the training time, we propose PCA, a dimensionality reduction method to reduce the feature space dimension. We compare our simulation results, in terms of accuracy and time taken for classification respectively, with the algorithms reported in other works.

Our contribution in this paper include

- The design and implementation of CLDNN, a combination of convolution neural network, long short term memory network and dense network for classifying the various modulation schemes used in beyond 5G wireless systems.
- Deriving of the hyper-parameters and model parameters using parameter tuning, namely gradient search, for the improvement of network's performance in terms of classification accuracy.
- Classification of 10 modulation schemes, which was not addressed in the literature, is made possible with the proposed work.
- Introduction of "mean cumulative sum" (MCS) pooling after ReLU operation at the convolutional layers.
- Implementation of principal component analysis to reduce the dimension of feature vectors and thereby to reduce the time taken for training.
- Considering the frequency selective fading in the channel model and obtaining the corresponding accuracy curve.
- Analysing the system interms of accuracy with respect to varying distance between transmitter and receiver.
- Deriving the closed form expression of bit error rate analysis of BPSK system after applying the modulation classification.

3 CLDNN based modulation classification

The proposed modulation classification system is shown in Fig. 1, in which the transmitter transmits $s(t;u_i)$. The baseband signal received at the receiver is $r(t)$ and is fed to the analog-to-digital converter (ADC) followed by the principal component analysis (PCA). The proposed system can be described in terms of a system model. The complex envelope of a received baseband signal is given by

$$r(t) = s(t;u_i) + n(t) \tag{1}$$

where $n(t)$ denotes complex gaussian noise and $s(t;u_i)$ in (1) is given by,

$$s(t;u_i) = b_i e^{j2\pi\Delta f t} e^{j\phi} \sum_{k=1}^{k} e^{j\theta_k} g_k^{(i)} p\,(t-(k-1)\,T-\xi T)\,; \quad 0 \le t \le KT \tag{2}$$

where ϕ denotes the time variant carrier phase introduced by propagation delay, Δf denotes an offset carrier frequency, θ_k phase jitter, $\left\{g_k^{(i)}\ ;\ 1 \le k \le K\right\}$ denotes K complex symbols taken from the i^{th} modulation format-symbol period and ξ denotes normalized epoch for the time offset between the transmitter and receiver respectively.

The output of principal component analysis is of reduced dimension and the same is given to the proposed CLDNN whose output is the classified modulation type denoted as $\hat{g}_k^i$. The classified modulation type is fed to the decoder along with the output of ADC for bit decoding. The output of decoder is denoted as $\hat{b}_i$.

3.1 Architecture of CLDNN

The proposed architecture consist of convolutional neural network, LSTM and dense network as shown in Fig. 2. This kind of combined architecture will provide high performance comparing to the traditional single-model based architecture. The reason for combining the models include, the convolutional neural network provides excellent feature extraction, as it is used along with the pooling layer at the first stage of the proposed architecture. A CNN with L layers holding L connections between every layer and its forthcoming layer, will have $L\frac{(L+1)}{2}$ direct connection as shown in Fig. 3. For every layer, the preceding layers' feature maps are used as input, and its own feature-maps are fed as inputs to all other forthcoming layers. LSTM provides superior performance for time series data through connection of previous state information to the present state [23]. Since our modulated signals are time series data, the architecture of LSTM as shown in Fig. 4 is introduced in the second stage to extract temporal feature set which is required for the modulation classification.

The DenseNet architecture which is shown in Fig. 5 is a logical extension of residual neural network (ResNet). This architecture has an Identity block to pass previous layer information (feature set) into many of the next coming future layers where those feature information can be merged by the additive block in the layer. This makes the next

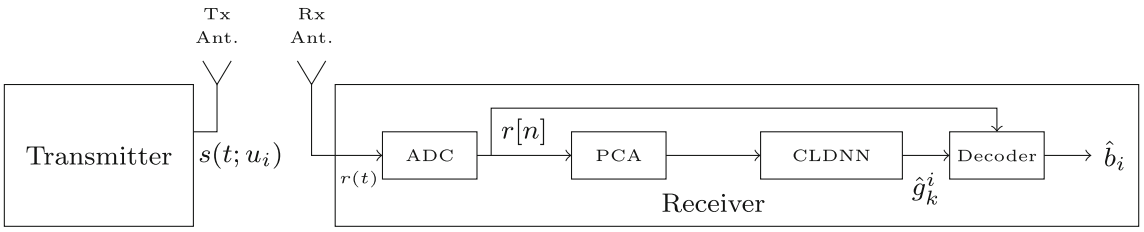

Fig. 1 Block diagram of proposed system

future layers to learn the residuals of previous layers (errors i.e. diff between some previous layer and current one). It avoids the future layers relearn redundant feature maps [12]. The jumped connection into next upcoming layer makes the network substantially deeper, more accurate, and efficient to train because of the shorter connections between layers close to the input and those close to the output.

The DenseNet shown in Fig. 5 will improve the flow of gradients and information for a complete network which made the training easier. It also observed that this dense connectivity gives regularized effects with smaller training set sizes which reduces the overfitting on tasks. This type of DenseNets also enable us to mitigate the vanishing-gradient problem, strengthen feature propagation, allows feature reuse, and reduce the number of required parameters.

Moreover, we introduce mean cumulative sum pooling after ReLU operation. The mean cumulative sum pooling is explained with respect to the sample data set shown in Fig. 6. The dataset is represented as a matrix of size 4 x 4 and if the same is flattened and denotes as $W = [2\ 4\ -1\ 1\ 2\ 8\ 3\ -2\ 1]$ for a stride of 1 and the filter size of $f = 3$, then its mean cumuative sum pooling is introduced as $M = \frac{1}{N}\sum_{j=0}^{N-1}(N-j)W_j$ and the same is given as 10.7778. The other values are also calculated and they are shown in Fig. 6

In nutshell, the combined architecture of convolutional layer network, LSTM and dense network along with the mean cumulative sum pooling proposed here will make the architecture more efficient, in terms of improved performance by incorporating the advantages of the convolutional layer network, LSTM and dense network. The architecture parameters are given in Table 1.

3.2 Dimensionality reduction through principal component analysis

Principal component analysis (PCA) is the simplest of the true eigenvector-based multivariate analyses [13]. It can be considered as one of the techniques of revealing the internal structure of the data in a way that it can best describe the variance of the data. If a multivariate data can be visualized as an object in a multi dimensional plane, then PCA can represent the picture in a reduced lower dimensional space by using only the major contributing eigenvector. This can be achieved by using only the first few principal components, so that the dimension of the data is reduced.

PCA is more analogous to the factor analysis. Factor analysis does more domain oriented assumptions about the associated structure and solves eigenvectors of a matrix which is slightly different. In this manner, PCA mitigates the number of dimensions represented by the input vectors.

The application of PCA in our classification scheme is shown in Fig. 7, in which the training or test data are given to the data centering block that subtracts mean from the data. The mean subtracted data is used to obtain the covariance matrix, followed by its computation of eigen vector and eigen value. From the calculated eigen vectors, the predominant vectors that contain modt of the information

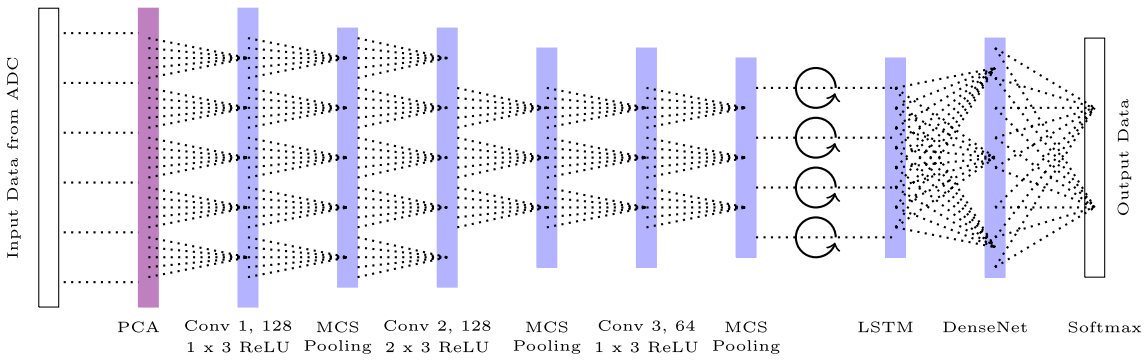

Fig. 2 CLDNN architecture

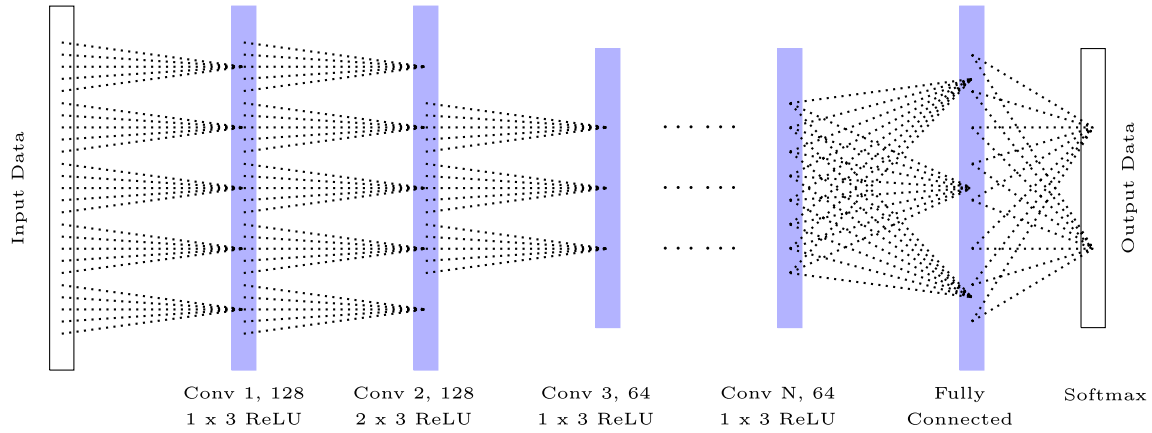

Fig. 3 Typical convolutional neural network from [11]

are retained. These principal component vectors alone are fed to the CLDNN architecture for clasification purpose. We apply PCA for all the input training vectors that correspond to different modulation schemes. In this way, we find the basis vectors for the reduced dimensional subspace corresponding to the training data followed by their projections on to these bases corresponding to the subspace. Since the number of bases vectors representing the input pattern is minimized, the corresponding training time will also be reduced in a linear pattern.

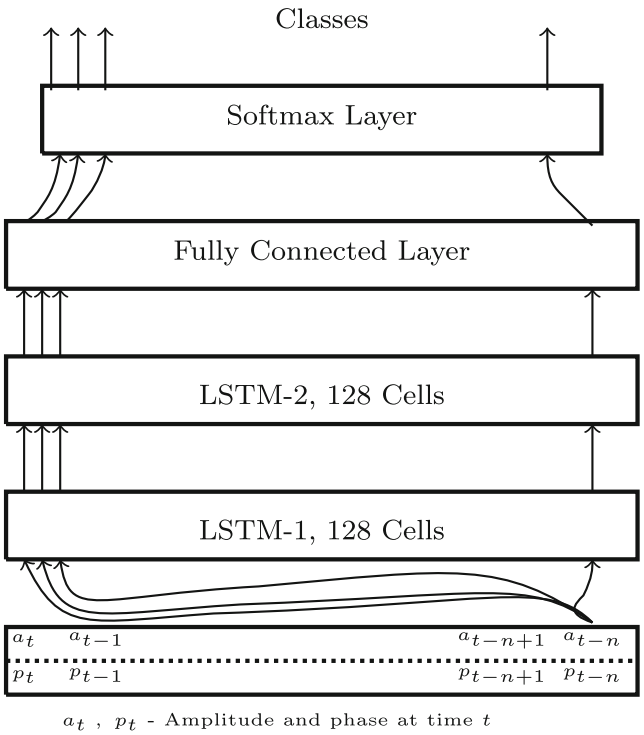

Fig. 4 Typical LSTM architecture from [23]

4 Dataset

The dataset generated and kept in RadioML2016.10b is used in our work. Total number of samples available in the dataset are 1200000. The dataset contains ten different modulations including 8 digital modulations namely, QAM64, QAM16, 8PSK, QPSK, BPSK, CPFSK, BFSK, PAM 4 and two analog modulations viz. AM-DSB and WB-FM (Table 2). For digital modulations, the dataset is uncorrelated to ensure that they become equi-probable bits and symbols. A continuous voice data is used as input in analog modulation. The voice data usually contains acoustic speech with some interludes and off times.

The data set is equally divided among all modulation types. The noises namely thermal noise and multipath fading were also included in the simulation. The channel model generation include noise model, sample rate offset model and fading model, center drift model. The sample rate of 1M sample per second is used to vectorize and pack the segmented output stream data of each simulation.

A sliding window that extracts 128 samples with a stride of 64 samples is used to form tha data set for our problem. In the GNU-radio library, there are 1200000 samples generated. These are segmented using 128 samples rectangular window for training and testing. The examples of 128 samples size are given to the LSTM network in polar form. The signal-to-noise ratio are evenly distributed in the dataset from -20dB to 18dB with the step size of 2 dB along with the labels.

4.1 Training and testing

Training and testing is conducted at the Keras library on the Theano backend. We used a Dell R740 workstation with Tesla V100 as the GPU to speed up the computation. The

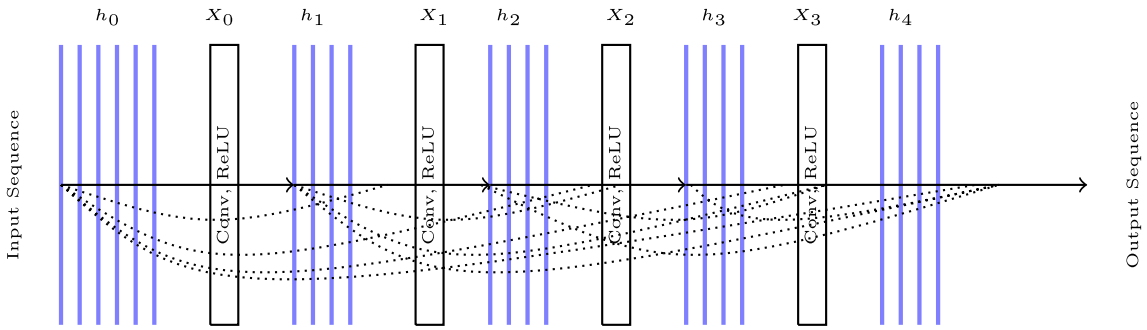

Fig. 5 Typical DenseNet architecture from [12]

Fig. 6 Sample Dataset and the result after MCS pooling

2	4	-1	3
1	2	8	5
3	-2	1	3
7	5	4	1

→

10.7778	13.333
14.222	16.2222

Table 1 CLDNN model architecture parameters

Stage 1		
First layer	Convolution 1	128 kernels with 1x3 ReLU with MCS pooling
Second layer	Convolution 2	128 kernels with 2x3 ReLU with MCS pooling
Third layer	Convolution 3	64 kernels with 1x3 ReLU with MCS pooling
Stage 2		
Fourth layer	LSTM	128 cells
Stage 3		
Fifth layer	DenseNet	64 kernels with ReLU

Fig. 7 Principal componenet analysis followed by CLDNN

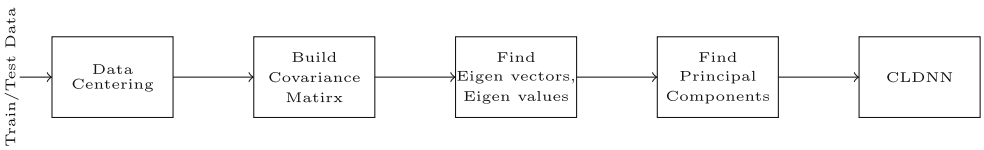

Table 2 Dataset attributes

Dataset parameter	Specification
No of Samples	1200000
Number of Modulations	10
Modulation Types	CPFSK, BFSK, 16QAM, QPSK, BPSK, 8PSK, 64QAM, PAM4, AM-DSB, and WB-FM
Temporal Resolution	128 micro seconds each
Sampling Rate	1 Msamp/sec

70% of the data sets are used for training and the remaining 30% are used for testing and validation. That is 840000 samples are used for the training and 360000 samples are utilized for testing.

The parameters are selected optimally based on machine learning parameter selection scheme. The learning rate was set to 0.0018, and we have used Adam optimizer. The batch size was chosen to be 1024 and the ReLU activation function was used for all layers. The convolution layers use a filter of size 3 and a stride of 1 with no zero padding. The mean cumulative sum pooling is used in the convolutional layers after ReLU operation. The activation that was used in the last layer is softmax activation function. The error function used was of categorical cross entropy function. Call

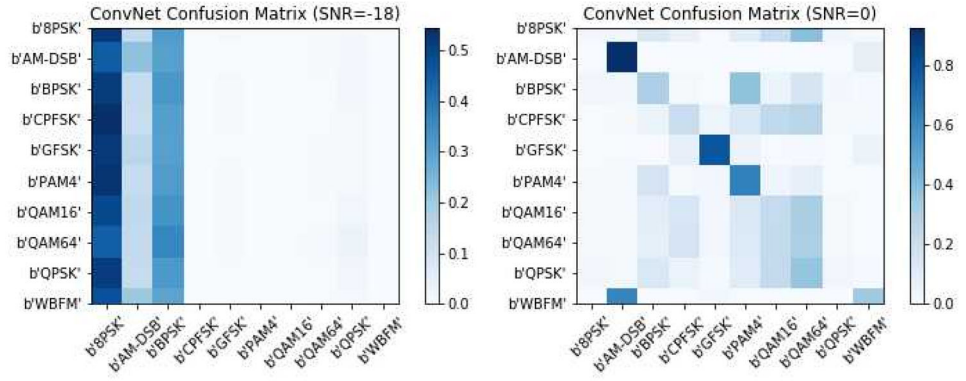

(a) Confusion matrix of CNN when SNR is -16 dB.

(b) Confusion matrix of CNN when SNR is 0 dB.

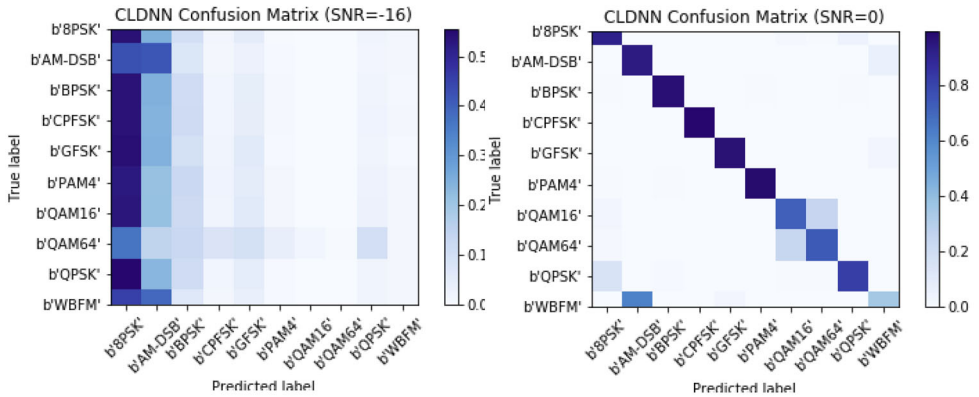

(c) Confusion matrix of CLDNN when SNR is -16 dB.

(d) Confusion matrix of CLDNN when SNR is 0 dB.

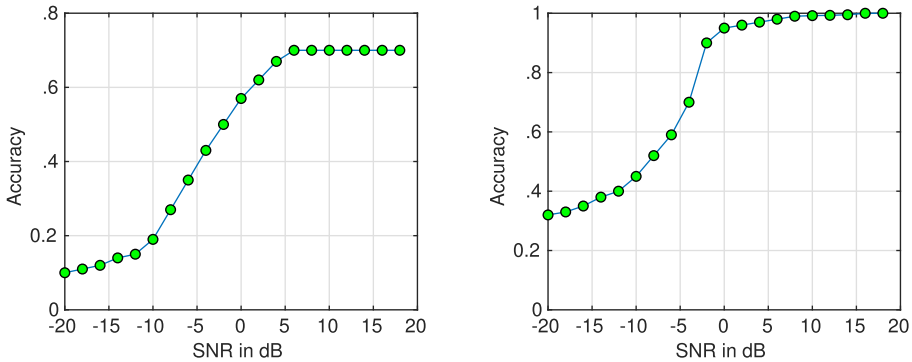

(e) Accuracy curve of CNN.

(f) Accuracy curve of CLDNN.

Fig. 8 Performance of CNN and CLDNN in terms of confusion matrix and accuracy curve

back function will be executed when the loss value does not show any improvement, so that the training will be stopped early.

5 Results and discussions

The simulation results for each of the network presented in the previous sections are discussed in this section in detail.

5.1 Convolutional neural network

The simulation results of CNN, whose architecture is shown in Fig. 3 are presented in this section in terms of confusion matrix and accuracy. The CNN with four layers is chosen for simulation. The results are shown in Fig. 8a, b and c respectively. We use 70% (840000) of the samples for the training and 30% (360000) of the samples for the testing. The data is spread all over the SNR ranges from -20 dB to 18 dB. The confusion matrix at the SNR value -18 dB is shown in Fig. 8a. The result clearly indicates a less performance accuracy, as the SNR is very low. However, there is a prominent improvement in the classification, when the SNR is increasing.

When the SNR is increasing, we see the diagonal nature of confusion matrix, for a few of the modulation types, namely "8-PSK", "AM-DSB", "BPSK", "CPFSK", and "GFSK". However, the classification accuracy gets reduced for other modulation types, even in high SNR. This can be seen in the non-diagonal nature of the confusion matrix of Fig. 8b for these modulation types alone. This is the reason we adapt CLDNN architecture for the efficient classification.

The accuracy curve as a function of varying SNR is shown in Fig. 8e. From the curve, we see that the maximum accuracy achieved is only 72%, even at the high SNR. These results clearly indicate the need of some better architecture for the modulation classification. So, we prefer CLDNN along with MCS pooling, whose accuracy improvement is discussed in the next section.

5.2 CLDNN

In this section, we discuss in detail about the simulation results of CLDNN in terms of its confusion matrix and accuracy. To simulate, we use 70% (840000) samples for training and 30% (360000) of the samples for testing. The training and testing data sets contain samples that are evenly distributed from -20 dB SNR to +18 dB SNR. The classification results of our first model, the four-layer CLDNN, are presented in the form of confusion matrices as shown in Fig. 8c and d respectively.

In situations where the signal power is below the noise power, as for the case when the SNR is -20dB, it is hard for CLDNN to extract the desired signal features, while when SNR grows above 0 dB, there is a prominent diagonal in the confusion matrix, denoting that most modulations are correctly recognized.

As seen in the Fig. 8c and d, the average classification accuracy is achieved by CLDNN when the SNR is larger. This fact seems to be obvious when we look at its confusion matrix, as there is a clean diagonal. We see from Fig. 8d, the strong diagonal entries for the modulation types, namely "BPSK", "AM-DSB", "CPFSK", "GFSK" and "PAM", which is not seen in Fig. 8c.

We have plotted in Fig. 8f, the prediction accuracy of CLDNN as a function of SNR. The accuracy obtained by CLDNN is 98% when the SNR reaches -1 dB. This clearly indicates an improvement from normal CNN, in which the maximum accuracy is only 72% as seen in Fig. 8e.

The simulation of accuracy with respect to SNR in frequency selective fading channel is presented in Fig. 9a.

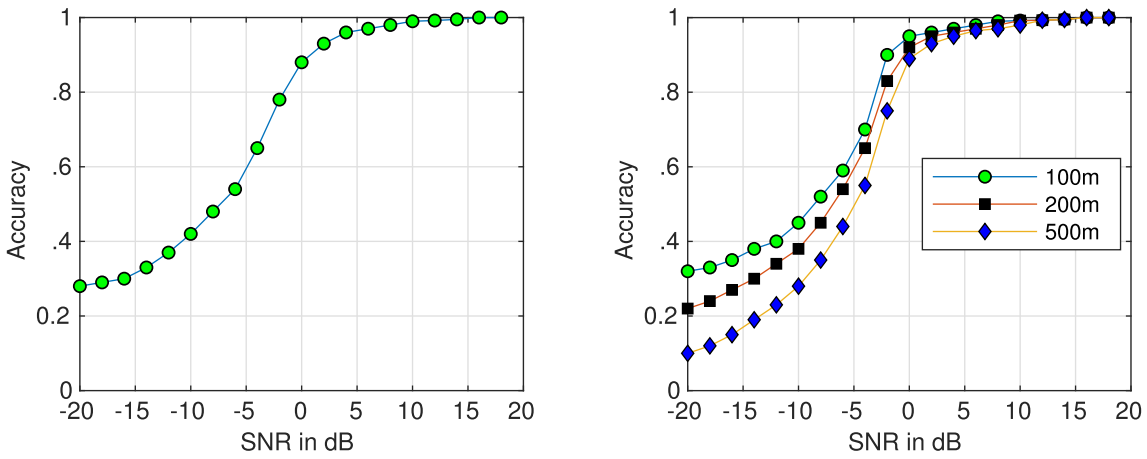

Fig. 9 Accuracy of CLDNN in frequency selective fading channel and with the varying distance between transmitter and receiver

We used GNU radio to generate the data for training. We have set number of taps randomly verying between 4 and 7 with tap delays uniformly generated between 0 and 10 μs, and normalized tap gains uniformly verying between 0 dB and -5 dB respectively. We have considered all types of modulations mentioned in the previous sections for generating the training data.

It is observed from Fig. 9a that the accuracy is slightly decreased while comparing with that of Fig. 8f. The reason for this decrease is obvious as frequency slective fading channel affects each frquency component differently.

We have presented the simulation results in Fig. 9b for the varying distance between transmitter and receiver. To simulate the results shown in Fig. 9b, we have considered

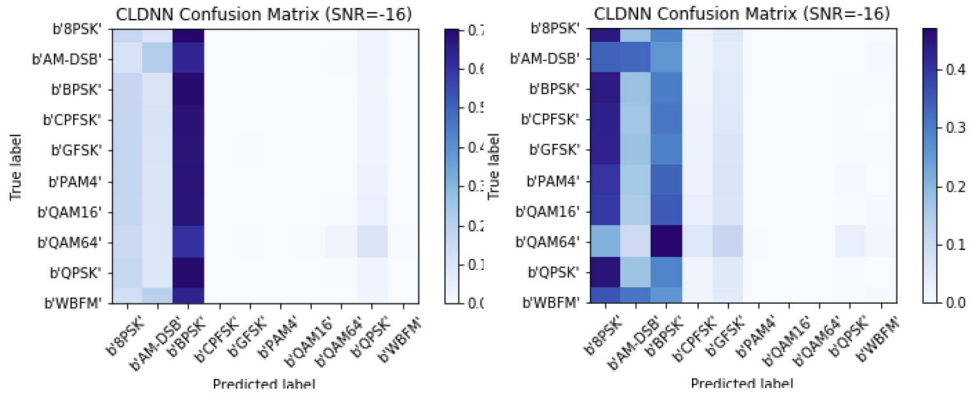

(a) Confusion matrix of CLDNN when SNR is -16 dB, after applying PCA to have 4 feature vectors

(b) Confusion matrix of CLDNN when SNR is -16 dB, after applying PCA to have 8 feature vectors

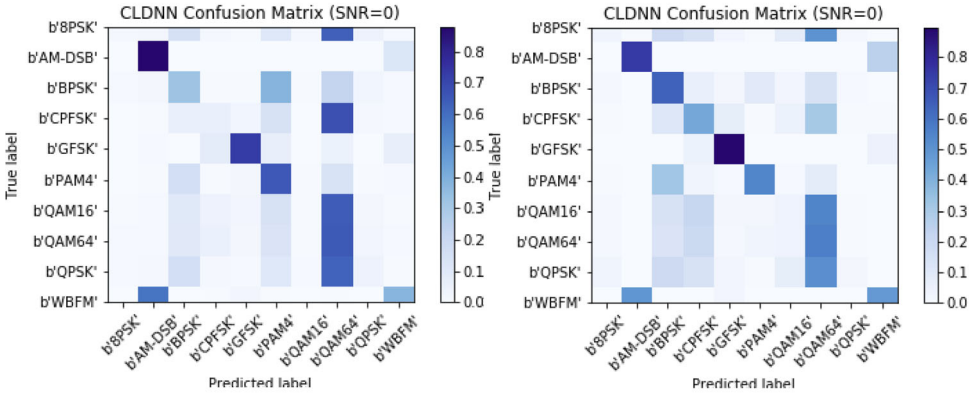

(c) Confusion matrix of CLDNN when SNR is 0 dB, after applying PCA to have 4 feature vectors

(d) Confusion matrix of CLDNN when SNR is 0 dB, after applying PCA to have 8 feature vectors

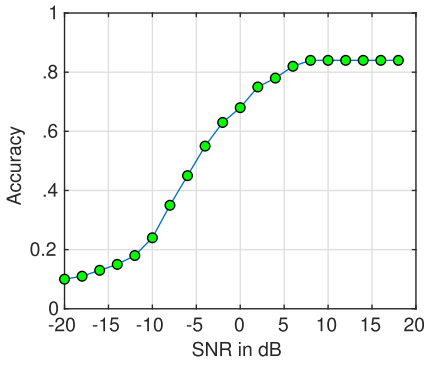

(e) Accuracy curve of CLDNN, after applying PCA to have 4 feature vectors

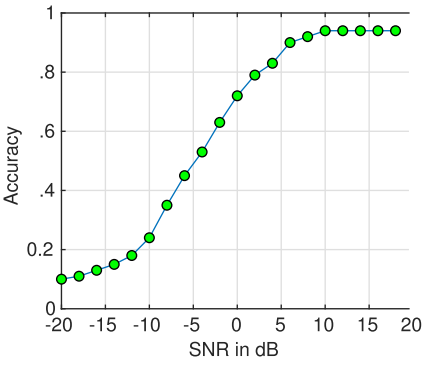

(f) Accuracy curve of CLDNN, after applying PCA to have 8 feature vectors

Fig. 10 Performance of CLDNN - after dimensionality reduction - in terms of confusion matrix and accuracy curve for various numbers of feature space reduction

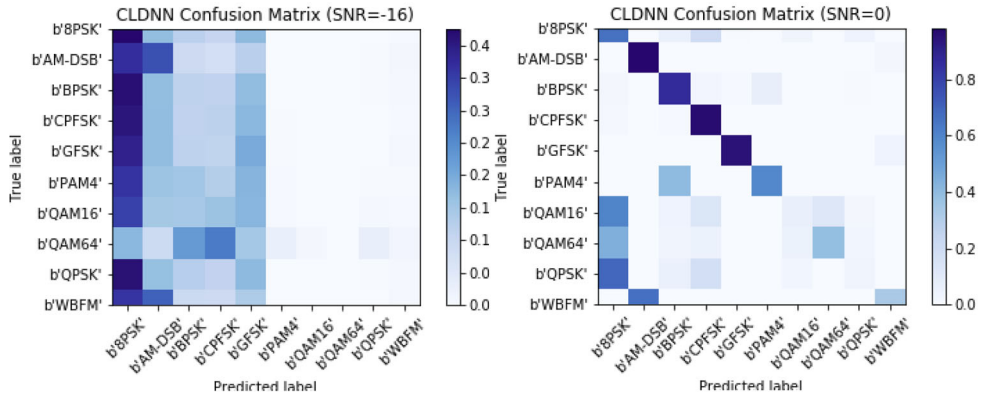

(a) Confusion matrix of CLDNN when SNR is -16 dB, after applying PCA to have 64 feature vectors

(b) Confusion matrix of CLDNN when SNR is 0 dB, after applying PCA to have 64 feature vectors

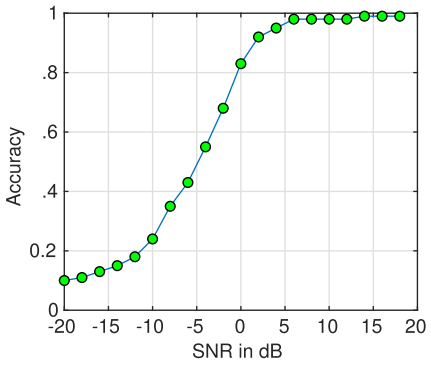

(c) Accuracy curve of CLDNN, after applying PCA to have 64 feature vectors

Fig. 11 Performance of CLDNN - after dimensionality reduction to have 64 feature vectors - in terms of confusion matrix and accuracy curve

the varying distance between the transmitter and receiver, such as 100m, 200m and 500m respectively. The accuracy curves were obtained for varying distances and plotted for comparison purposes. From Fig. 9b, it is observed that when the distance between transmitter and receiver increases, the accuracy decreases, which is clearly visible at low SNR. However, in high SNR regions, the deviation in accuracy is very negligible.

5.3 Dimensionality reduction

The simulation results of CLDNN after dimensionality reduction is presented in this section. We consider reducing the dimension to have the feature size of 4, 8 and 64 respectively. We consider 70% (840000) of the samples for training and 30% (360000) of the samples for testing respectively. The results in terms of confusion matrix and accuracy after reducing the dimension to the size of 4 and 8 are shown in Fig. 10a, b, c and d respectively. The corresponding results after reducing the dimension to the size of 64 is shown in Fig. 11a and b respectively. The results are presented for the SNR value of -16 dB and 0 dB.

It is obvious from Figure that the confusion matrix looks half diagonal, when the SNR is high, for the feature dimensions reduced to the size of 4 and 8. Confusion matrix looks better when the number of dimensions after reduction is larger. In other words, the "feature space reduced to 8" outperforms the case of "feature space reduced to 4". The case of "64 features" improves further as clearly seen in Fig. 11b.

The accuracy curve presented in Fig. 10e and f also verifies this argument, i.e., the maximum accuracy achieved in Fig. 10e is only 84%, whereas achieved in Fig. 10f is close to 94%. The performance is further improved in Fig. 11c, in which the accuracy is 99.8%. Though we compromise on accuracy to a minimum level, we are confident of reducing the training time, because when we run the algorithm without applying PCA in a system having GPU with Tesla V-100 processor, it took 8 hours, 27 minutes, 39 seconds, while after reducing the dimension using PCA, it took only 5 hours, 12 minutes, and 3 seconds. The plot between error and number of epoch is shown in Fig. 12, in which the error is plotted with respect to verying number of epochs and verifies the fact that error gets reduced when number of epoch is incresed and it reaches the

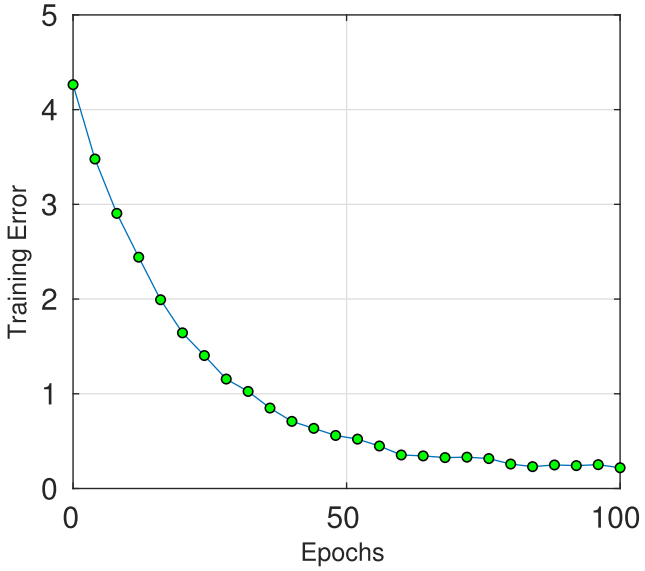

Fig. 12 Plot between error and number of epoch

value of 0.2 when epoch is 100. It also ensures that the loss function decreases during the process of weight updation.

5.3.1 Bit error rate analysis

In this section, we would like to present the bit error rate performance analysis. We have shown the simulation results of bit error rate of BPSK system alone after successful modulation classification in Fig. 13. The mathematical analysis of bit error rate is as follows

The received signal in BPSK system can be written as

$$y = x + n + P\epsilon \tag{3}$$

where $x \in \{-A, A\}$, $n \sim C\mathcal{N}(0, \sigma^2)$, $\sigma^2 = N_0$. In (3), ϵ is modelled as complex term representing the error due to wrong modulation classification as $\epsilon \sim \mathcal{U}(-A, A) + j\mathcal{U}(-A, A)$, because of which, wrong constellation is identified during detection, where $\mathcal{U}$ denotes uniform discrete random number, and P denotes the factor depending on accuracy, which lies between 0 and 1, *i.e.*, $P = 1-\mathrm{a}$, a denotes accuracy. If P is 1, then an error always is introduced in the constellation, and if P is 0, then no error in constellation is introduced. The mean and variance of ϵ can be easily verified to be $0 + j0$ and $2P^2$ respectively.

Using central limit theorem, the addition of noise and error due to poor accuracy can be modelled as complex gaussian with real and imaginary parts

$$\eta_{re} = n_{re} + \epsilon_{re} \sim \mathcal{N}\left(0, \frac{\sigma^2}{2} + P^2\right) \tag{4}$$

$$\eta_{im} = n_{im} + \epsilon_{im} \sim \mathcal{N}\left(0, \frac{\sigma^2}{2} + P^2\right) \tag{5}$$

So, the bit error probability is

$$P_b = P\{\eta > A\} = \int_A^\infty \frac{1}{\sqrt{2\pi\left(\frac{\sigma^2}{2} + P^2\right)}} e^{\frac{-x^2}{2\left(\frac{\sigma^2}{2} + P^2\right)}} dx \tag{6}$$

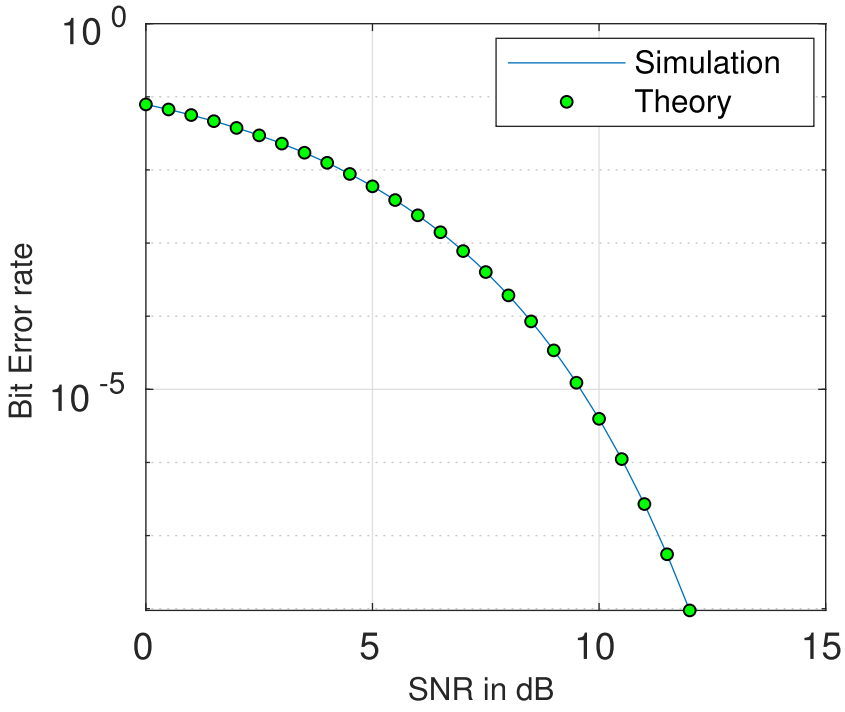

Fig. 13 Bit error rate analysis of BPSK system after modulation classification using CLDNN

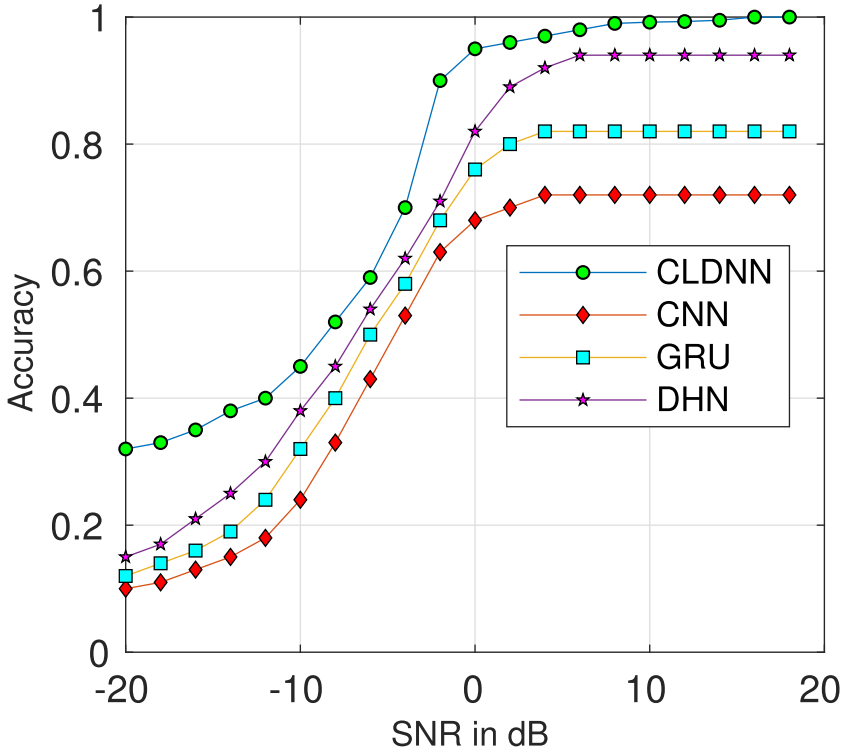

Fig. 14 Accuracy of CLDNN - a comparision with simple CNN, deep hierarchical network, and GRU

The equation can be simplified as

$$P_b = \mathcal{Q}\left(\frac{A}{\sqrt{\frac{\sigma^2}{2} + P^2}}\right) \tag{7}$$

where $\mathcal{Q}(\cdot)$ is a Q function. The bit error rate performance of BPSK system is shown in Fig. 13, in which we have assumed that the accuracy is 0.99, so that $P = 0.01$. We have varied the SNR from 0 dB to 12 dB and modelled the BPSK system with modulation classification error, because of $P = 0.01$. It is verified from Fig. 13 that the bit error rate is 1×10^{-5}, when the SNR is 10 dB, which is very minimum.

The comparision between the accuracy of CLDNN, a simple CNN, a gated recurrent unit (GRU) network presented in [8] and deep heiarchical network presented in [18] is shown in Fig. 14. It is clear from Fig. 14 that the CLDNN outperforms simple CNN, which is very obviuos, as the proposed architecture incude LSTM and densenet in addition to the simple CNN. It is also noted that CLDNN outperforms GRU network presented in [8]. Moreover the performance is slightly better than that of deep hierarchical network proposed by [18].

6 Conclusion

In this paper, the CLDNN - a combination of architectures of convolutional neural network, long short term memory and dense network is presented to classify various modulations used in "beyond 5G" wireless systems. Also, we have introduced mean cumulative sum based pooling layer after ReLU operation in the convolutional layers of CLDNN. The performance of the proposed architecture is verified in terms of the classification accuracy and confusion matrix. It is also shown that the proposed network outperforms an ordinary convolutional neural network in terms of its accuracy. Inorder to reduce the training time, we have used PCA for dimensionality reduction. The results verify that even with the reduced dimensional feature vector, the algorithm is able to achieve 99.8% of classification accuracy. In the future work, we would like to test the system for a varying distance between the transmitter and the classifying receiver. Moreover, we would like to consider the mobility scenario in the classification algorithm.

References

1. Abu-Romoh M, Aboutaleb A, Rezki Z (2018) Automatic modulation classification using moments and likelihood maximization. IEEE Commun Lett 22(5):938–941
2. Blanquez-Casado F, Torres MDCA, Gomez G (2019) Link adaptation mechanisms based on logistic regression modeling. IEEE Commun Lett 23(5):942–945
3. Chen W, Xie Z, Ma L, Liu J, Liang X (2019) A faster maximum-likelihood modulation classification in flat fading non-gaussian channels. IEEE Commun Lett 23(3):454–457

4. Daldal N, Polat K, Guo Y (2019) Classification of multi-carrier digital modulation signals using ncm clustering based feature-weighting method. Comput Ind 109:45–58
5. Güner A., Alçin ÖF, Şengür A (2019) Automatic digital modulation classification using extreme learning machine with local binary pattern histogram features. Measurement 145:214–225
6. Hatzichristos G, Fargues MP (2001) A hierarchical approach to the classification of digital modulation types in multipath environments. In: Conference record of thirty-fifth asilomar conference on signals, systems and computers (Cat. No. 01CH37256), vol 2. IEEE, pp 1494–1498
7. He K, Zhang X, Ren S, Sun J (2016) Deep residual learning for image recognition. In: Proceedings of the IEEE conference on computer vision and pattern recognition, pp 770–778
8. Hong D, Zhang Z, Xu X (2017) Automatic modulation classification using recurrent neural networks. In: 2017 3rd IEEE international conference on computer and communications (ICCC). IEEE, pp 695–700
9. Hong L, Ho K (1999) Identification of digital modulation types using the wavelet transform. In: MILCOM 1999. IEEE Military Communications. Conference Proceedings (Cat. No. 99CH36341), vol 1. IEEE, pp 427–431
10. Huq KMS, Busari SA, Rodriguez J, Frascolla V, Bazzi W, Sicker DC (2019) Terahertz-enabled wireless system for beyond-5g ultra-fast networks: a brief survey. IEEE Netw 33(4):89–95
11. Huynh-The T, Hua CH, Kim DS (2019) Learning action images using deep convolutional neural networks for 3d action recognition. In: 2019 IEEE sensors applications symposium (SAS). IEEE, pp 1–6
12. Kamel M, Hamouda W, Youssef A (2016) Ultra-dense networks: a survey. IEEE Commun Surv Tutorials 18(4):2522–2545
13. Li JM, Hu YH, Tao XH (2005) Recognition method based on principal component analysis and back-propagation neural network. Infrared and Laser Engineering 34(6):719
14. Li W, Dou Z, Qi L, Shi C (2019) Wavelet transform based modulation classification for 5g and uav communication in multipath fading channel. Phys Commun 34:272–282
15. Mingquan L, Xianci X, Lemin L (1998) Ar modeling-based features extraction of multiple signals for modulation recognition. In: ICSP'98. 1998 Fourth international conference on signal processing (Cat. No. 98TH8344), vol 2. IEEE, pp 1385–1388
16. Mobasseri BG (2000) Digital modulation classification using constellation shape. Signal Processing 80(2):251–277
17. Nie J, Zhang Y, He Z, Chen S, Gong S, Zhang W (2019) Deep hierarchical network for automatic modulation classification. IEEE Access 7:94,604–94,613
18. Nie J, Zhang Y, He Z, Chen S, Gong S, Zhang W (2019) Deep hierarchical network for automatic modulation classification. IEEE Access 7:94,604–94,613
19. Nolan KE, Doyle L, O'Mahony D, Mackenzie P (2001) Modulation scheme recognition techniques for software radio on a general purpose processor platform. In: Proceedings of the first joint IEI/IEE symposium on telecommunication systems, Dublin
20. O'Shea TJ, Corgan J, Clancy TC (2016) Convolutional radio modulation recognition networks. In: International conference on engineering applications of neural networks. Springer, pp 213–226
21. Parvez I, Rahmati A, Guvenc I, Sarwat AI, Dai H (2018) A survey on low latency towards 5g: ran, core network and caching solutions. IEEE Commun Surv Tutorials 20(4):3098–3130
22. Polydoros A, Kim K (1990) On the detection and classification of quadrature digital modulations in broad-band noise. IEEE Trans Commun 38(8):1199–1211
23. Sainath TN, Vinyals O, Senior A, Sak H (2015) Convolutional, long short-term memory, fully connected deep neural networks. In: 2015 IEEE international conference on acoustics, speech and signal processing (ICASSP). IEEE, pp 4580–4584
24. Shah MH, Dang X (2020) Low-complexity deep learning and rbfn architectures for modulation classification of space-time block-code (stbc)-mimo systems. Digital Signal Processing 99(102):656
25. Sills J (1999) Maximum-likelihood modulation classification for psk/qam. In: MILCOM 1999. IEEE Military Communications. Conference Proceedings (Cat. No. 99CH36341), vol 1. IEEE, pp 217–220
26. Sills J (1999) Maximum-likelihood modulation classification for psk/qam. In: MILCOM 1999. IEEE Military Communications. Conference Proceedings (Cat. No. 99CH36341), vol 1. IEEE, pp 217–220
27. Swami A, Sadler BM (2000) Hierarchical digital modulation classification using cumulants. IEEE Trans Commun 48(3):416–429
28. Wang Y, Wang J, Zhang W, Yang J, Gui G (2020) Deep learning-based cooperative automatic modulation classification method for mimo systems. IEEE Trans Veh Technol 69(4):4575–4579
29. Xue R, Hu D, Zhu T (2017) Application of adaptive coded modulation technology in uav data link. Int J Commun Netw Sys Sci 10(5):181–190
30. Zhang D, Ding W, Liu C, Wang H, Zhang B (2020) Modulated autocorrelation convolution networks for automatic modulation classification based on small sample set. IEEE Access 8:27,097–27,105

Publisher's note Springer Nature remains neutral with regard to jurisdictional claims in published maps and institutional affiliations.

Dr. J. Christopher Clement received his PhD degree in the area of wireless communication and M.E degree in communication systems from Vellore Institute of Technology and Anna university respectively. He is a certified data scientist and he has been teaching for more than 15 years. He has authored a book titled "Cognitive Radio". At Present, he is with the School of Electronics Engineering, VIT University, India, as an Associate Professor. His research interest is in machine learning, deep learning, statistical signal processing and cognitive radio communication.

N. Indira was born in Krishnagiri, Tamil Nadu, India. She received her Bachelor's Degree in Electronics and Communication Engineering from Coimbatore Institute of Technology, Coimbatore in 2011 and Master's Degree in Communication Engineering from Vellore Institute of Technology, Vellore in 2020. Her research interest in Wireless Communication, especially in LTE and 5G technology.

Dr. P. Vijayakumar has completed his Ph.D. from SRM IST (2018) in applied machine learning in wireless communication (cognitive radio), Master in Applied Electronic from the college of engineering, Guindy (2006), and B.E (ECE) from Madras University (2000). He is a Certified "IoT specialist" and "Data scientist". He is a recipient of the NI India Academic award for excellence in research (2015). His current research interests are in the area of Machine and Deep learning, IoT based intelligent system design, Blockchain technology, and cognitive radio networks. He is a senior member of IEEE. He is currently working as an Associate Professor in the ECE Department, SRM IST, Chennai, Tamil Nadu, and India.

Dr. R. Nandakumar received his B.E degree in Electronics and Communication Engineering and M.E. degree in Applied Electronics from K.S.Rangasamy college of Technology, Namakkal, India in 2000 and 2006 respectively. He received the Ph.D. degree in Faculty of Information and Communication from Anna University, Chennai, India in 2017. Presently he is Professor & Head in Department of ECE, K S R Institute for Engineering and Technology, Namakkal, India. His research interests include Medical image Processing, Medical Electronics and Machine learning.